Pseudocapacitive Charge Storage in Layered Oxides $SrLaFe_{1-x}Co_xO_{4-\delta}$ (x = 0 - 1)

Md. Sofiul Alom[1], Farshid Ramezanipour[1,]*

[1]Department of Chemistry, University of Louisville, Louisville, KY 40292, USA

*Corresponding author. farshid.ramezanipour@louisville.edu, +1(502) 852-7061

ORCID: 0000-0003-4176-1386

Abstract

Pseudocapacitive energy storage has been demonstrated for three materials belonging to a family of layered oxides. This work is the first report on the observation of charge-storage properties in this family of materials that feature 2-dimensional layers, consisting of MO_6 units (M = transition metal). The spaces between layers are occupied by alkaline-earth or rare-earth metals. Systematic trends have been demonstrated, where the charge-storage properties are enhanced as a function of Co-concentration, structural distortion and oxygen-deficiency in $SrLaFe_{1-x}Co_xO_{4-\delta}$. Symmetric pseudocapacitor cells based on these materials show substantial specific capacitance, energy density and power density. They are also remarkably stable and retain their charge storage capacity even after 1000 cycles of charge-discharge. The observation of pseudocapacitive charge-storage properties in these materials indicates the potential of this class of layered oxides for utilization in energy storage.

Keywords: pseudocapacitor, layered oxides, oxide-intercalation

1.Introduction

Supercapacitors offer high power density, but suffer from low energy density, which hinders their practical applications. To achieve both high energy density and power density, pseudocapacitors have received much attention. This is because conventional double-layer capacitors store energy by non-Faradaic processes, but pseudocapacitors utilize Faradaic charge transfer, leading to enhanced energy density.[1] In addition, pseudocapacitors maintain high power density because the Faradaic processes occur near the surface and do not depend on bulk diffusion. There are different types of pseudocapacitors, i.e., underpotential deposition, redox, and intercalation pseudocapacitors. In the latter category, the charge transfer occurs by intercalation and deintercalation of ions.[2-3] The intercalation of oxide anion in some ABO_3-type perovskite oxides has been observed, e.g., $La_{1-x}Sr_xBO_3$ (B = Fe, Mn, Co),[4] $LaNi_{1-x}Fe_xO_{3-\delta}$,[5] $La_{1-x}Ca_xMnO_3$,[6] and $SrCo_{0.9}Nb_{0.1}O_3$.[7] In this work, we explore the pseudocapacitive charge storage through oxide intercalation in a series of layered oxides, which are structural analogues of the fluoride K_2NiF_4. The three layered oxides studied here have formula, $SrLaFeO_4$, $SrLaCo_{0.5}Fe_{0.5}O_4$, and $SrLaCoO_{4-\delta}$. Some properties of these compounds have been studied before.[8-16] However, to our knowledge, this is the first report of the pseudocapacitive energy storage in this family of materials.

2.Experimental

The three compounds were synthesized through solid-state method at 1300 °C. The structures[8,12-13] (Figure 1) were confirmed by Rietveld refinements using powder X-ray diffraction (Figure S1). Electrochemical studies were done using a three-electrode electrochemical workstation and a symmetric two-electrode cell. Details of the synthesis and characterization procedures are provided in the Supporting Information.

3.Results and Discussion

The structure of these materials is analogous to that of the fluoride K_2NiF_4, with general formula A_2MO_4. In the three compounds studied in this work, the M-sites are occupied by Fe/Co that form single layers of $(Fe/Co)O_6$ octahedra. These layers are separated by Sr^{2+} and La^{3+}. The three compounds are isostructural. Table S1 lists a representative set of the refined structural parameters. The oxygen content of these materials was determined by iodometric titration, which indicated 4 oxygens per formula unit for $SrLaFeO_4$ and $SrLaCo_{0.5}Fe_{0.5}O_4$, but 3.8 oxygens per formula unit for $SrLaCoO_{4-\delta}$.

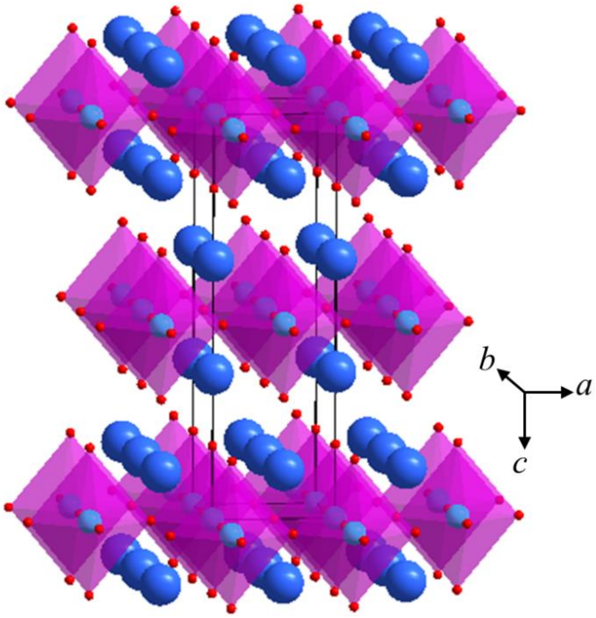

Figure 1. Crystal structure of $SrLaFe_{1-x}Co_xO_{4-\delta}$. Purple octahedra are $(Fe/Co)O_6$ units and large blue spheres represent Sr and La.

Figure 2a-c show the cyclic voltammetry (CV) data at different scan rates, 5, 10, 20, 40, 60, 80, and 100 mV/s. The presence of redox peaks and quasi-rectangular CVs are indicative of pseudocapacitive properties.[2,4-7,17-18] Two pairs of redox peaks are observed for $SrLaCoO_{4-\delta}$, corresponding to $Co^{2+\leftrightarrow 3+}$ and $Co^{3+\leftrightarrow 4+}$ redox processes.[4, 7] The two pairs of peaks for $SrLaFeO_4$

are less pronounced and correspond to Fe$^{2+\leftrightarrow 3+}$ and Fe$^{3+\leftrightarrow 4+}$ redox events,[4] while for $SrLaCo_{0.5}Fe_{0.5}O_4$ the redox peaks of Fe and Co overlap.

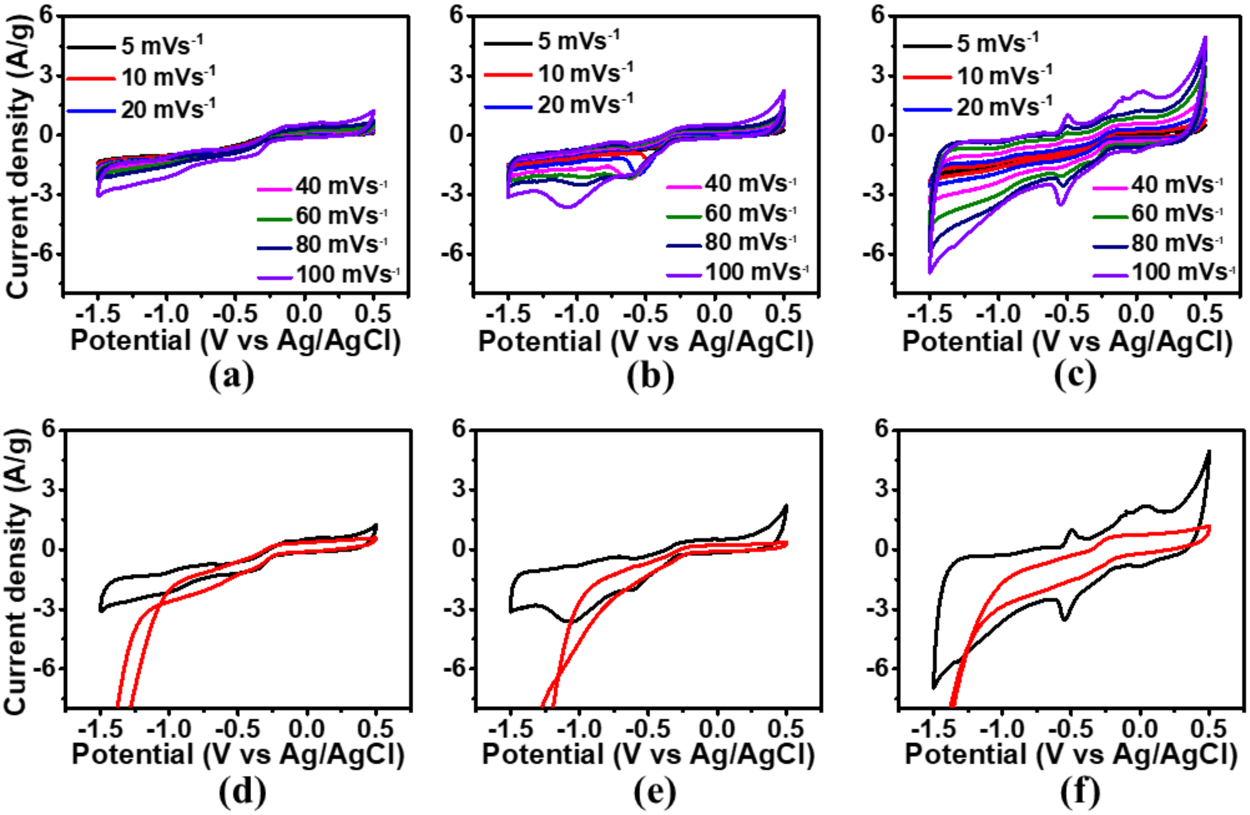

(a) (b) (c)

(d) (e) (f)

Figure 2. Cyclic voltammetry data for $SrLaFeO_4$ (a), $SrLaCo_{0.5}Fe_{0.5}O_4$ (b), and $SrLaCoO_{4-\delta}$ (c) in 1M KOH, in a potential window of -1.5 to 0.5 V vs Ag/AgCl. Parts d – f show the CVs in 1M KOH (black) and 1M KNO_3 (red) at 100mV/s for $SrLaFeO_4$, $SrLaCo_{0.5}Fe_{0.5}O_4$, and $SrLaCoO_{4-\delta}$, respectively.

As described for other pseudocapacitors, these redox processes occur due to the intercalation of oxide anion. The mechanism of oxide anion intercalation has been described before,[2,18] where the hydroxide ion from the electrolyte is adsorbed on the electrode surface, then loses a proton to another hydroxide ion to produce water. The oxide anion that is left behind, is intercalated into the electrode material.[2,18] To confirm that redox events are a function of the hydroxide ion concentration, we repeated the experiments in 1M KNO_3. Figure 2d-f show a comparison of CVs in 1M KOH and 1M KNO_3. The pronounced redox peaks that occur in 1M KOH, are not present in 1M KNO_3, indicating that redox reactions are facilitated by hydroxide ion, leading to oxide anion intercalation.[2]

It is evident from the presence of both anodic and cathodic peaks that the Faradaic processes are reversible.[19] At higher scan rates, the oxidation peaks shift slightly to higher potentials and reduction peaks to lower potentials. These shifts, that are commonly observed in pseudocapacitors, are a result of the internal resistance of the electrode[20-21] and indicate that the charge transfer kinetics is the limiting step.[22] In addition, the peak intensities increase at higher scan rates, which indicates fast electronic and ionic transport.[18,22] Furthermore, the facile mass transport and electron conduction are evident from the retention of the CV shapes at different scan rates,[18,21-22] while the CV areas increase at higher scan rates.

A symmetric two-electrode cell was constructed to investigate the galvanostatic charge-discharge (GCD) using these pseudocapacitors in the potential window of 0.0 to 1.7 V. Figure 3a shows the GCD cycles at 1A/g, exhibiting the expected triangular shape, typical of pseudocapacitors.[6,17] Specific capacitance is calculated from GCD curves using the following equation:[1,23]

$$C_s = \frac{4I\,\Delta \mathrm{t}}{m\,\Delta \mathrm{V}}$$

where I is the constant applied current, ΔV is the window of the potential response, Δt is the discharge time, and m is the total mass of the active material loaded on both electrodes. The GCD experiment was conducted at a wide range of current densities, from 0.5 A/g to 20 A/g, and the specific capacitance was calculated at each current destiny. As shown in Figure 3b, the specific capacitance decreases at higher current densities, as commonly observed in pseudocapacitors.[6, 17]

This is due to the internal resistance of the electrode, which at higher current densities, limits the utilization of the pseudocapacitor material.[6,17] The specific capacitance at 0.5A/g is 4.9 F/g for $SrLaFeO_4$, 5.5 F/g for $SrLaCo_{0.5}Fe_{0.5}O_4$, and 19.9 F/g for $SrLaCoO_{4-\delta}$. The latter shows superior specific capacitance to some of the previously reported anion-based pseudocapacitors, such as $La_{1-x}Ca_xMnO_3$ showing ~13 F/g (that rapidly diminishes to ~2 F/g) at 0.5 A/g [6] and $La_{1-x}Sr_xMnO_3$ with ~7.75 F/g at 0.5 A/g.[17]

As stated before, the best performing compound in the series, $SrLaCoO_{4-\delta}$, contains oxygen-deficiency, whereas the other two compounds have 4 oxygens per formula unit. $SrLaCoO_{4-\delta}$ also has the smallest unit cell and greatest distortion in MO_6 octahedral units (M = transition metal), where the equatorial bonds in the *ab* plane are significantly shorter than the axial bonds in the *c* direction (Table S2).

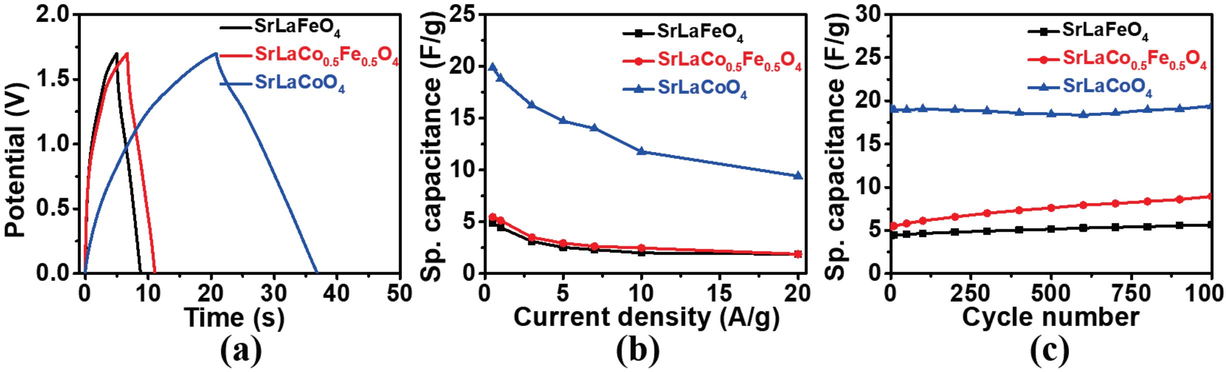

Figure 3. (a) GCD profile at 1A/g in 1M KOH. (b) Variation of specific capacitance as a function of current density. (c) Stability tests over 1000 cycles at 1A/g in 1M KOH.

To obtain the energy density of a cell, the following equation is used:[24]

$$E = \frac{C_s V^2}{2 \times 3.6}$$

where C_s is the specific capacitance obtained from the two-electrode cell and V is the potential window. The constant $\frac{1}{3.6}$ is used to calculate the energy density in Wh/kg, considering that 1W =

1V × 1A and 1F = 1 $\frac{s\,A}{V}$. The value of energy density (E), can then be used to calculate the power density using the following equation:[24]

$$P = \frac{E \times 3600}{\Delta t}$$

where Δt is the discharge time in seconds and 3600 is a multiplier used to obtain the power density in W/kg. $SrLaFeO_4$, $SrLaCo_{0.5}Fe_{0.5}O_4$, and $SrLaCoO_{4-\delta}$ can deliver energy densities of 1.96 Wh/kg, 2.19 Wh/kg, and 7.98 Wh/kg at power density of 850 W/kg from a symmetric cell when the applied current density is 0.5 A/g. $SrLaCoO_{4-\delta}$ shows the best energy and power density. In comparison, a symmetric cell of a previously reported anion-based pseudocapacitor, $La_{1-x}Ca_xMnO_3$, delivers energy density of ~2.6 $Whkg^{-1}$ at power density of ~800 Wkg^{-1} for current density of 0.5 A/g.[6] Another reported system, $La_{1-x}Sr_xMnO_3$, provides an energy density of ~1.55 $Whkg^{-1}$ at power density of 1000 Wkg^{-1} for 0.5 A/g.[17]

Another important parameter for pseudocapacitors is their stability over numerous cycles. Therefore, we investigated the stability of these materials over 1000 cycles of GCD at a current density of 1A/g. As shown in Figure 3c, these materials are remarkably stable and maintain a nearly constant specific capacitance after 1000 cycles.

We note that further studies and improvements are needed for practical applications. However, the current study is important from fundamental science perspective, as it reports the first example of pseudocapacitive properties in layered K_2NiF_4-type oxides, as well as systematic trends as a function of structural distortion, oxygen-deficiency, and electronic structure of transition metals.

Acknowledgement

This work is supported in part by the National Science Foundation under Grant No. DMR-1943085.

References

[1] R. Vellacheri, A. Al-Haddad, H. Zhao, W. Wang, C. Wang, Y. Lei, Nano Energy 8 (2014) 231-237.

[2] J. T. Mefford, W. G. Hardin, S. Dai, K. P. Johnston, K. J. Stevenson, Nat. Mater. 13 (2014) 726-732.

[3] S. B. Karki, F. Ramezanipour, ACS Appl. Energy Mater. 3 (2020) 10983-10992.

[4] C. T. Alexander, J. T. Mefford, J. Saunders, R. P. Forslund, K. P. Johnston, K. J. Stevenson, ACS Appl. Mater. Interfaces 11 (2019) 5084-5094.

[5] C. T. Alexander, R. P. Forslund, K. P. Johnston, K. J. Stevenson, ACS Appl. Energy Mater. 2 (2019) 6558-6568.

[6] H. Mo, H. Nan, X. Lang, S. Liu, L. Qiao, X. Hu, H. Tian, Ceram. Int. 44 (2018) 9733-9741.

[7] L. Zhu, Y. Liu, C. Su, W. Zhou, M. Liu, Z. Shao, Angew. Chem. Int. Ed. 55 (2016) 9576-9579.

[8] N. Qureshi, H. Ulbrich, Y. Sidis, A. Cousson, M. Braden, Phys. Rev. B 87 (2013) 054433.

[9] L. Xu, Y.-M. Yin, N. Zhou, Z. Wang, Z.-F. Ma, Electrochem. Commun. 76 (2017) 51-54.

[10] D. Singh, S. Singh, A. Mahajan, N. Choudhary, Ceram. Int. 40 (2014) 1183-1188.

[11] S. Gupta, M. K. Verma, D. Singh, Ceram. Int. 42 (2016) 18418-18424.

[12] H. El Shinawi, C. Greaves, J. Solid State Chem. 181 (2008) 2705-2712.

[13] R. Ang, Y. P. Sun, X. Luo, C. Y. Hao, W. H. Song, J. Phys. D: Appl. Phys. 41 (2008) 045404.

[14] Q. W. Yao, X. L. Wang, Z. X. Cheng, G. Peleckis, S. X. Dou, R. Nigam, G. P. Zhao, J. Appl. Phys. 101 (2007) 09N515.

[15] Y. Y. Liu, X. M. Chen, X. Q. Liu, Solid State Commun. 136 (2005) 576-579.

[16] X. Yang, L. Luo, H. Zhong, Catal. Commun. 6 (2005) 13-17.

[17] X. Lang, H. Mo, X. Hu, H. Tian, Dalton Trans. 46 (2017) 13720-13730.

[18] W. Che, M. Wei, Z. Sang, Y. Ou, Y. Liu, J. Liu, J. Alloys Compd. 731 (2018) 381-388.

[19] X. W. Wang, Q. Q. Zhu, X. E. Wang, H. C. Zhang, J. J. Zhang, L. F. Wang, J. Alloys Compd. 675 (2016) 195-200.

[20] J. Yan, Z. Fan, W. Sun, G. Ning, T. Wei, Q. Zhang, R. Zhang, L. Zhi, F. Wei, Adv. Funct. Mater. 22 (2012) 2632-2641.

[21] J. Zhang, H. Liu, P. Shi, Y. Li, L. Huang, W. Mai, S. Tan, X. Cai, J. Power Sources 267 (2014) 356-365.

[22] D. Guo, H. Zhang, X. Yu, M. Zhang, P. Zhang, Q. Li, T. Wang, J. Mater. Chem. A 1 (2013) 7247-7254.

[23] M. D. Stoller, R. S. Ruoff, Energy Environ. Sci. 3 (2010) 1294-1301.

[24] T. Kshetri, D. T. Tran, D. C. Nguyen, N. H. Kim, K.-t. Lau, J. H. Lee, Chem. Eng. J. 380 (2020) 122543.